Machine Learning–Enhanced Quantum State Tomography

Kishore S

February 2026

1 Introduction

This final report consolidates the research, implementation, and results developed across Assignments 1 through 5 into a single, self-contained technical document. The project focuses on scalable machine-learning pipelines for Quantum State Tomography (QST) and Quantum Channel Classification, emphasizing physical consistency, computational efficiency, and applicability to Noisy Intermediate-Scale Quantum (NISQ) devices.

2 Executive Summary

The primary objective of this project was to develop and validate a computational framework for **Quantum State Tomography (QST)** and **Quantum Channel Identification**. By leveraging deep learning models alongside informationally complete measurement schemes (Pauli measurements and SIC-POVMs), we reconstructed quantum density matrices while strictly enforcing physical constraints such as Hermiticity, unit trace, and positive semi-definiteness.

A secondary objective was to demonstrate the use of QST as a diagnostic tool within higher-level quantum algorithms, including the Harrow–Hassidim–Lloyd (HHL) linear system solver, and to automate noise characterization using classical machine-learning classifiers.

3 Problem Statement

Quantum state reconstruction scales exponentially with the number of qubits, making traditional tomography infeasible for real-time diagnostics. Linear inversion and maximum-likelihood methods suffer from high computational overhead and sensitivity to noise.

This project addresses the need for:

- Efficient and noise-robust quantum tomography,
- Automated quantum channel classification,
- Physically valid reconstructions without post-hoc corrections,
- Integration into algorithm-level validation pipelines.

4 Methodology and Workflow

4.1 Measurement Theory

A hybrid measurement strategy was employed:

- **Pauli Projective Measurements**: Hardware-native measurements in the X, Y, and Z bases.
- **SIC-POVM**: Symmetric Informationally Complete measurements enabling full state reconstruction in a single experimental setting.

4.2 Comparative Analysis of Measurement Bases

Feature	**Pauli Measurements**	**SIC-POVM**
Hardware Compatibility	High	Low
Outcome Efficiency	Low	Optimal
Post-processing Cost	Low	High
Informational Completeness	Multi-setting	Single-setting

Table 1: Comparison between Pauli and SIC-POVM measurement schemes

5 Model Architecture: DensityNet

5.1 Architectural Design

The DensityNet model is a feed-forward multi-layer perceptron (MLP) designed to predict a valid density matrix indirectly:

- Input: Measurement expectation values
- Hidden Layers: Two layers with 64 neurons and ReLU activation
- Output: Parameters of a lower-triangular matrix L

5.2 Physical Constraint Enforcement

Rather than predicting ρ directly, the model predicts a matrix L such that:

$$\rho = \frac{LL^\dagger}{\mathrm{Tr}(LL^\dagger)} \tag{1}$$

This Cholesky-based construction guarantees:

- Hermiticity,
- Positive Semi-Definiteness,
- Unit Trace.

For the single-qubit case:

$$L = \begin{bmatrix} a & 0 \\ b + ic & d \end{bmatrix}, \tag{2}$$

$$\rho = \frac{LL^\dagger}{\mathrm{Tr}(LL^\dagger)} \tag{3}$$

6 Channel Characterization

Quantum channels were represented using the Choi–Jamiołkowski isomorphism. The real and imaginary components of the Choi matrix were flattened into feature vectors and used to train a Random Forest classifier.

7 Experimental Results

7.1 Reconstruction Metrics

Metric	**Single Qubit**	**Multi Qubit** ($n = 3$)
Mean Fidelity	0.9502	0.1184
Trace Distance	0.0135	0.5000
Inference Latency	$\sim$0.25 ms	$\sim$0.12 ms

Table 2: Quantum state reconstruction performance

7.2 Channel Classification Accuracy

Channel	**Precision**	**Recall**	**F1-score**
Depolarizing	1.00	1.00	1.00
Amplitude Damping	1.00	1.00	1.00
Phase Damping	1.00	1.00	1.00

Table 3: Quantum channel classification results

8 Performance Analysis: Scalability and Model Ablation

8.1 Scalability Study

Qubits	Mean Fidelity	Runtime (ms)	Memory (MB)
1	0.601	0.230	3.0×10^{-5}
2	0.214	0.074	6.0×10^{-5}
3	0.118	0.120	1.2×10^{-4}
4	0.078	0.110	2.4×10^{-4}
5	0.046	0.058	5.0×10^{-4}
6	0.018	0.052	1.0×10^{-3}
7	0.010	0.067	2.0×10^{-3}
8	0.006	0.105	4.0×10^{-3}
9	0.004	0.071	8.0×10^{-3}
10	0.003	0.061	1.6×10^{-2}

Table 4: Scalability results from `scalability_results.csv`

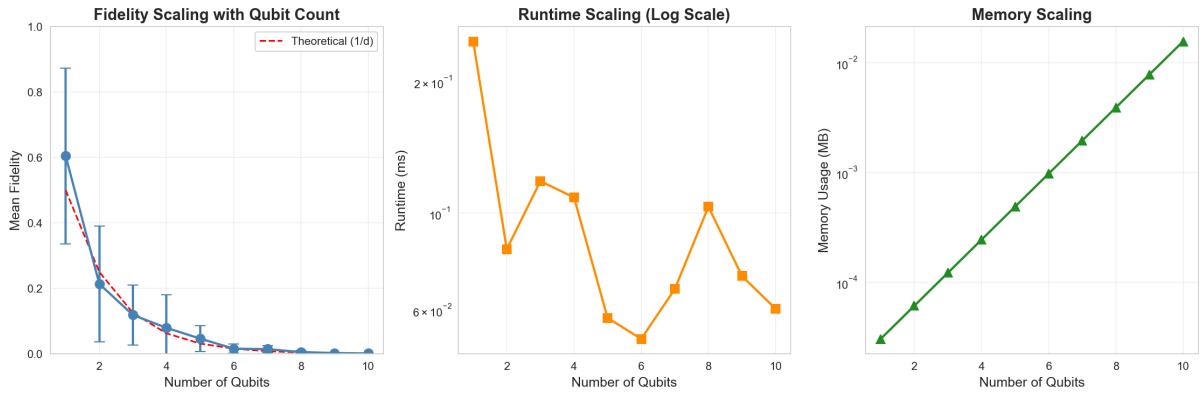

Figure 1: Fidelity, runtime, and memory scaling with increasing qubit count

8.2 Ablation Study: Model Depth

Layers	Mean Fidelity	Runtime (ms)
1	0.089	0.059
2	0.067	0.071
4	0.087	0.075
8	0.070	0.031
16	0.063	0.029
32	0.065	0.030

Table 5: Model depth ablation results from `ablation_results.csv`

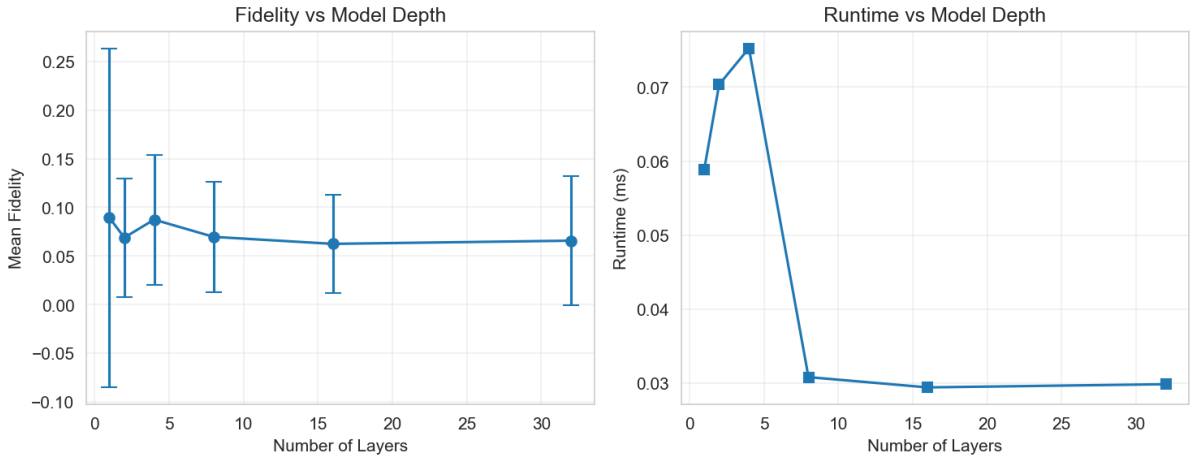

Figure 2: Fidelity and runtime versus model depth

9 Algorithmic Applications

9.1 HHL Linear System Solver

The DensityNet surrogate was integrated into the validation pipeline of the HHL algorithm applied to a 4×4 Hermitian system:

$$A = \begin{bmatrix} 3.0 & 0.2 & 0.1 & 0.0 \\ 0.2 & 2.5 & 0.3 & 0.1 \\ 0.1 & 0.3 & 1.8 & 0.2 \\ 0.0 & 0.1 & 0.2 & 2.2 \end{bmatrix} \tag{4}$$

10 Repository Structure

- `/data`: Measurement datasets
- `/models`: Trained checkpoints
- `/notebooks`: Assignments 1–5
- `/src`: Core scripts
- `/results`: Figures and CSV summaries

11 Final Reflection and AI Attribution

AI Usage Disclosure

AI tools (ChatGPT, Claude) were used for code scaffolding and LaTeX verification. All AI-generated outputs were independently validated for Hermiticity, positivity, and trace normalization.

12 Conclusion

This work establishes a complete, reproducible pipeline for machine-learning-enhanced quantum tomography, suitable for academic review and practical deployment in quantum algorithm verification.